Chinese Journal of Polymer Science Vol. 34, No. 2, (2016), 185–194

Chinese Journal of Polymer Science

Highly Stretchable and Self-healing Hydrogels Based on Poly(acrylic acid) and Functional POSS*

Liu-qing Yang, Lu Lu**, Chao-wen Zhang and Chang-ren Zhou**
Department of Materials Science and Engineering, Jinan University, Guangzhou 510632, China

Abstract Herein, we present a novel way for the production of self-healing hydrogels with stretch beyond 4200% than their initial length and relatively high tensile strength (0.1–0.25 MPa). Furthermore, the hydrogel was insensitive to notch. Even for the samples containing V-notches, a stretch of 2300% was demonstrated. The hydrogels were developed by *in situ* crosslinking of the self-assembled colloidal poly(acrylic acid) (PAA)/functionalized polyhedral oligomeric silsesquioxane (POSS) micelles. This was achieved by the addition of functionalized polyhedral oligomeric silsesquioxane with tertiary amines and hydroxyls (POSS-AH) into the PAA reaction solution. The POSS-AH led to micellar growth, then the dual-crosslinked network was constructed. One type of crosslink was formed by hydrogen-bonding and ionic interactions between PAA chains and POSS-AH, the other type of crosslink was formed by covalent bonds between PAA and bis(*N*,*N*'-methylene-bis-acrylamide).

Keywords: Hydrogel; Highly stretchable; Self-healing; Poly(acrylic acid); Functionalized polyhedral oligomeric silsesquioxane.

INTRODUCTION

Hydrogels, infinite crosslinking polymer networks that absorb substantial amounts of aqueous solutions[1–3], closely resemble many soft tissues of the human body and their unique structure makes them attractive for biomedical applications[4–6], such as surgical implants, cartilage repair and drug delivery. For conventional hydrogels, their applications are often limited by the weak mechanical strength and reconstructive abilities[7, 8]. In the last few decades significant progress has been achieved in the development of hydrogels with enhanced mechanical properties, such as double-network hydrogels (DN gels)[9, 10], macromolecular microsphere composite hydrogels (MMC gels)[11], nanocomposite hydrogels (NC gels)[12], *ect*. Self-healing is an important characteristic observed in living systems. Self-healing materials would offer enormous possibilities, in particular for long-term reliability of implanted biomaterials[13]. Based on the concept of supramolecular chemistry[14, 15], self-healing gels have been developed through reconstructive covalent dangling side chain or non-covalent bondings such as hydrogen bonding[16], electrostatic interactions[17], molecular recognition[18], hydrophobic associations[19] and dual network designs[20–22]. Although supramolecular hydrogels display rapid self-healing ability without any stimulus, they always suffer from the poor mechanical strength, which prevents them from any stress-bearing applications such as cartilage and tissue engineering scaffolds[23].

Poly(acrylic acid) (PAA) hydrogels have the ability to absorb many times their weight in water and are

* This work was financially supported by the Natural Science Foundation of Guangdong Province (No. 2014A030313379) and the National Natural Science Foundation of China (Nos. 81171459 and 31400824).
** Corresponding authors: Lu Lu (鲁路), E-mail: tlulu@jnu.edu.cn or luxixi801@gmail.com
Chang-ren Zhou (周长忍), E-mail: tcrz9@jnu.edu.cn
Received August 7, 2015; Revised September 22, 2015; Accepted September 25, 2015
doi: 10.1007/s10118-016-1744-1

widely used as mucoadhesives[24] and controlled release devices[25] in biomedical field. In the past few years, several methods have been used to generate self-healing PAA hydrogels. Wei *et al*. prepared autonomous self-healing PAA hydrogels through the dynamic bonding of physical cross-linking and the migration of ferric ions[26]. Gulyuz *et al*. designed a novel way for the production of self-healing hydrogels with shape memory behavior and high mechanical strength. Hydrophobically modified PAA chains with cetyltrimethylammonium (CTA) counterions formed the physical network. Extraction of free cetyltrimethylammonium bromide (CTAB) micelles resulted in a drastic increase in their Young's moduli and tensile strengths due to the complex formation between PAA and CTAB[27]. However, the high concentration of Fe^{3+} or CTAB in these systems may not be desirable for biomedical applications.

In order to combine the high mechanical strength and self-healing properties together, functionalized polyhedral oligomeric silsesquioxane with tertiary amines and hydroxyls (POSS-AH) was introduced to PAA network in our study. POSS is one of the members in silsesquioxane family which has highly symmetric molecules with a nanoscopic size feature and can be considered as one of the best organic/inorganic hybrid nanomaterials. The unique structure and superior biocompatibility of POSS allow it to be used in many biomedical applications such as tissue engineering, drug delivery and biosensors[28]. By *in situ* crosslinking of the self-assembled colloidal PAA/POSS-AH micelles, the dual-crosslinked network was constructed. The mechanical properties, self-healing ability and swelling characterization were investigated. In addition, based on the experimental results, a possible mechanism for the formation of the dual crosslink network was speculated.

EXPERIMENTAL

Materials

Acrylic acid (AA, Tianjin Fuchen Chemistry reagents factory) was distilled under reduced pressure before use. *N*,*N*'-Methylenebisacrylamide (Bis, Amesco) and potassium persulfate ($K_2S_2O_8$, Tianjin Fuchen Chemistry Reagents Factory) were of analytical-reagent grade and were used as received without further purification.

The POSS-AH nanoparticles were prepared according to the procedure developed by Mori *et al*.[29] and the method was described in detail in our previous publication[30]. Briefly, the first step was the synthesis of *N*,*N*-di(2,3-dihydroxypropyl)-(aminopropyl) triethoxysilane. 1 mol of (aminopropyl) triethoxysilane was dropped slowly into 2 mol of glycidol under stirring with ice cooling and then reacted for 1 h at room temperature. The second step was the hydrolytic condensation of the step one product in methanol with HF under stirring. After an additional reaction for 2 h under stirring at ambient temperature, the methanol, ethanol and water were removed by the vacuum drying method (40 °C, 0.8 MPa, about 12 h). The final product POSS-AH was obtained in 80% yield.

Hydrogel Preparation

The hybrid hydrogel was prepared by *in situ* free radical polymerization. Firstly, AA aqueous solution was neutralized to a certain degree with sodium hydroxide solution (NaOH) in an ice bath then continuously stirred in order to prevent the self-initiated auto-polymerization. The AA concentration was 34 wt% after the neutralization. Secondly, POSS-AH and Bis at different molar ratios were added to the solution and stirred. After they all dissolved, 0.5% (weight percent relative to AA) $K_2S_2O_8$ was added as an initiator and the mixture was further stirred until a uniform solution was obtained. Finally, the solution was injected into a Teflon mold with lid. The polymerization was allowed to proceed for 2 h in a water bath at 60 °C.

Mechanical Test

All mechanical tests were performed at room temperature using a universal testing machine (AG-I, Shimadzu). The samples for tensile test were dumbbell-shaped (20 mm (L) × 4 mm (D) × 2–3 mm (W)) and the crosshead speed was set at 100 mm/min. The compression test was performed on cylinder samples (15 mm in diameter and (14 ± 0.5) mm in initial thickness) at a rate of 5 mm/min. The samples for tearing test were cut into the size of 30 mm (L) × 3 mm (D) and the length of the initial notch was 20 mm. Each sample was stretched at constant rate of 200 mm/min while the tearing force F was recorded.

Microstructure Observation

Field emission scanning electron microscope (FE-SEM, UltraTM55, Zeiss) with an energy dispersive spectrometry (EDS) modular was used for elemental analysis and the localization of POSS-AH nanoparticles in the hydrogels. The freeze-dried hydrogels were sputter coated with platinum then observed under FE-SEM.

The submicrometer structure of the nanocomposite hydrogels were observed by a transmission election microscope (TEM, Tecnai™G2 F30) working at 120 kV. Prior to the TEM characterization, the hydrogels were completely dried under vacuum at 60 °C for 24 h, and then cut into ~100 nm thick sections using an ultramicrotome (Leica, UC6/FC6) and placed onto copper grids.

Self-healing Experiments

The dumbbell-shaped POSS-PAAC hydrogels were cut by a blade into two halves, then the separated pieces were brought into contact with each other without application of any external force in closed containers at 37 °C. 24 h later the tensile tests were performed on as-prepared and self-healed gels. In this study the effects of different POSS-AH contents, AA concentrations and neutralized degrees of AA on performance of self-healing were investigated.

Swelling and Water Retention Test

Prior to swelling test the hydrogel samples were completely dried in a vacuum oven at 60 °C. For the swelling characterization, two types of solution were used: deionized water and normal saline (sodium chloride solution 0.9 wt%). The swelling ratio of the hydrogel as a function of time was measured as follows. Pre-weighted dried hydrogel (W_d) was immersed into solution, and the mass of the swollen hydrogel (W_s) was determined at regular intervals after removal of the surface water. The weight based swelling ratio (SR) was calculated by Eq. (1).

$$\mathrm{SR} = \frac{W_s - W_d}{W_d} \times 100\% \tag{1}$$

The water retention tests were performed to evaluate the water-conserved capacity of hydrogels. Fully swollen samples were placed in dishes at 37 °C and 80% relative humidity. The weight of fully swollen hydrogel (W_f), and hydrogel at each juncture (W_t) were recorded. The water retention ratio (WR) was defined by Eq. (2).

$$\mathrm{WR} = \frac{W_t}{W_f} \times 100\% \tag{2}$$

Three replicas were used for each sample composition, so that SR and WR results were expressed as average ± standard deviation.

RESULTS AND DISCUSSION

Mechanical Properties

To determine the mechanical performance of the PAA/POSS-AH hydrogels, uniaxial tensile and compression tests were conducted on a series of hydrogel samples prepared by adding two types of cross-linkers with various POSS-AH/Bis ratios. The hydrogels were denoted as P*n*B*m* at a constant crosslinker/AA ratio (9.6×10^{-3}% in mol), where P for POSS-AH and B for Bis, *m* and *n* was the percentage of POSS-AH and Bis respectively (in mol). The initial reactant compositions are listed in Table 1.

The tensile stress-strain curves are shown in Fig. 1(a). As the crosslinker ratio of POSS-AH was increased, the Young's modulus during elongation decreased while the elongation ratio at break increased. Sample P100 (only using POSS-AH as cross-linking agent) exhibited the highest elongation ratio beyond 4200% and the tensile strength was still greater than 0.1 MPa. POSS-AH with tertiary amines and hydroxyls worked as a multifunctional cross-linker and formed physically interactions between PAA polymer chains through hydrogen-bonding interaction and ionic complexation. By replacing some of the physical crosslink with covalent crosslink, the strength of the hydrogel was greatly enhanced. So the mechanical properties of PAA/POSS-AH hydrogel could be adjusted over a wide range simply by changing the proportion of physical and chemical cross-linkers.

Table 1. The initial reactant compositions of PAA/POSS-AH hydrogels

Samples	AA (mol/L)	NaOH [a] (%)	POSS [b] ($\times 10^{-3}$%)	Bis [c] ($\times 10^{-3}$%)
P100	5.5	75	9.6	0
P75B25	5.5	75	7.2	2.4
P50B50	5.5	75	4.8	4.8
P25B75	5.5	75	2.4	7.2
B100	5.5	75	0	9.6
P5	5.5	75	2.4	0.32
P10	5.5	75	4.8	0.32
A4.2	4.2	75	4.8	0.32
A5.5	5.5	75	4.8	0.32
A6.3	6.3	75	4.8	0.32
N50	5.5	50	4.8	0.32
N75	5.5	75	4.8	0.32
N85	5.5	85	4.8	0.32

[a, b, c] The molar ratios of NaOH, POSS-AH and Bis to AA, respectively
For all samples 0.5% (weight percent relative to AA) $K_2S_2O_8$ was used.

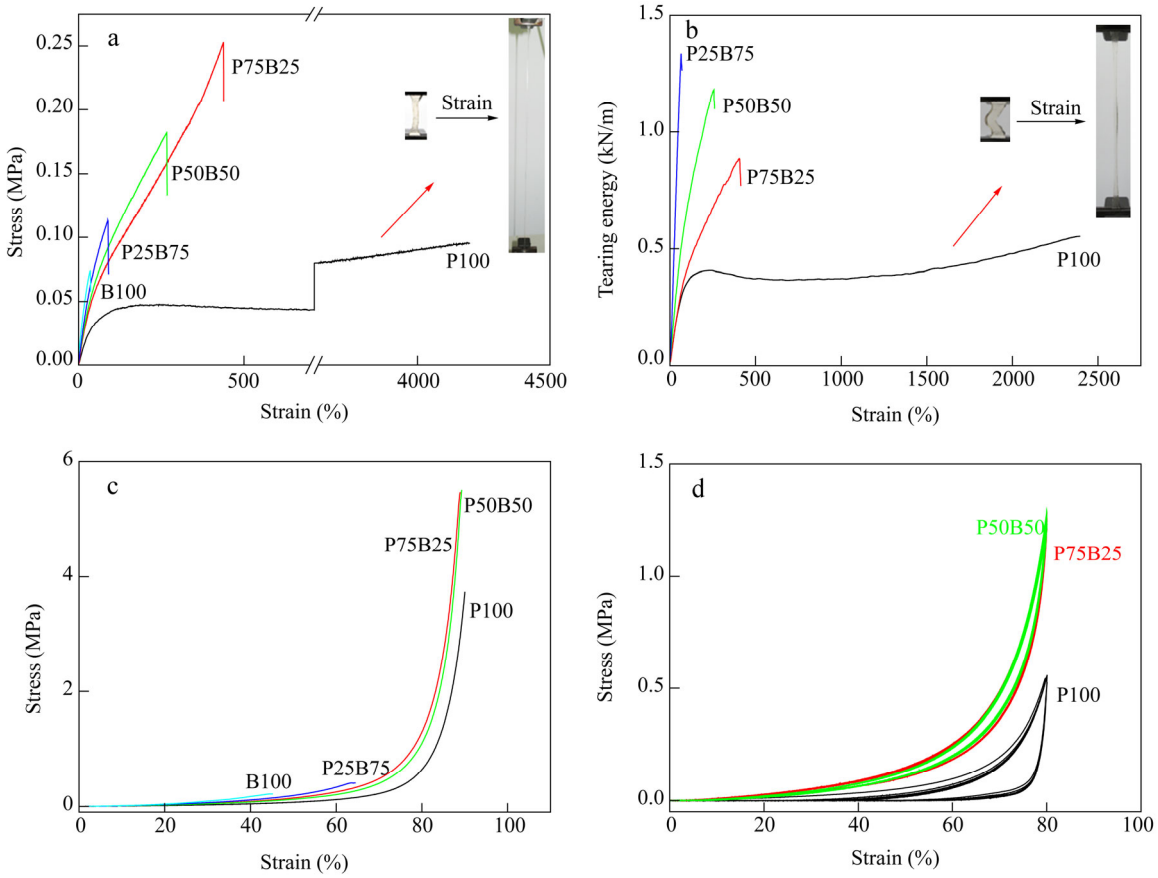

Fig. 1 Mechanical tests under various conditions: (a) tensile stress-strain curves, (b) tearing energy-strain curves, (c) compression stress-strain curves and (d) compression loading-unloading curves

The tearing test results illustrated that sample P100 was also extremely notch-insensitive. The V-notched sample P100 was stretched to 2300% of its initial length and remained stable, then the instrument reached the maximum range (Fig. 1b). These performances could be attributed to the complexation formed by the hydrogen-bonding and ionic interaction between PAA polymer chains and POSS-AH nanoparticles[31]. When the hybrid

hydrogel was extruded, the multi-arms physical crosslinks deformed and swung their arms. The random coil configuration of long chain polymers was fully stretched and the process absorbed a large amount of energy. Therefore the hydrogel exhibits high stretch ability and notch-insensitive properties.

The results of compression test (Fig. 1c) showed that the critical stress reached the maximum value when the molar ratio of POSS-AH to Bis was 1:1 but excessive chemical cross-linkers made the hydrogels brittle.

The resilience of the hydrogels was determined by cyclic compression test (Fig. 1d). Each sample was compressed to 80% of its original height for 5 run cycles. An obvious hysteresis that was found in the cycle curves of P100 suggested an effective energy-dissipating mechanisms exists in the network, which has been observed in several types of tough hydrogel[32]. The hysteresis decreased when some physical interactions were replaced by covalent crosslinks. Samples B100 and P25B75 were broken at the first cycle due to the fragility of the hydrogels caused by the high amount of covalent crosslinks.

Microstructure Analysis

The EDS spectrum (Fig. 2a) shows the peaks for carbon, oxygen, silicon and sulfur corresponding to their binding energies, respectively. Figure 2(b) illustrates the distribution pattern of the major elements. The results confirmed the homogeneous dispersion and distribution of Si throughout the crosslink network. The POSS-AH particles can be uniformly dispersed in water because of the high functionality[33]. Each silicon atom bound to one alkyl chain with the hydroxyl functionalities, so the silica particles can be uniformly dispersed in water and behave as single dissolved molecules to form a transparent colloidal solution. During the polymerization of AA, the physical crosslinks between POSS-AH and PAA chains can form *in situ*. The hydrogen bondings and ionic interactions between them also prevented unwanted agglomeration of the silica nanoparticles.

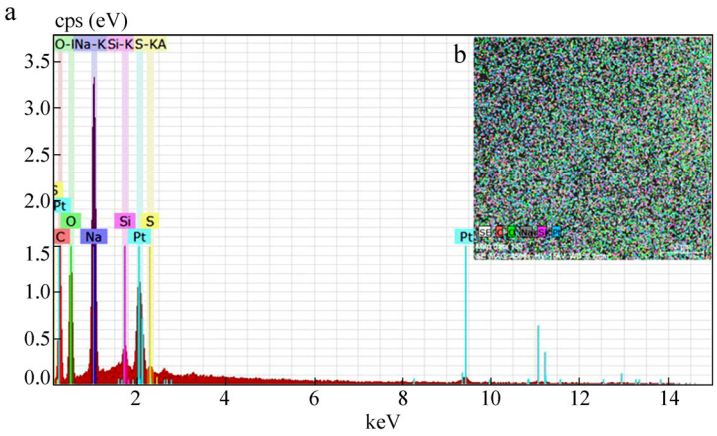

Fig. 2 EDS spectrum of sample P50B50

The submicrometer structure of the hydrogels was also observed by TEM. Petal-shaped clusters and flower-shaped spheres were observed (Fig. 3). Due to the different electron densities, carbon and hydrogen atoms present lower contrast than silicon atoms do under TEM. Based on this idea, the clusters in the TEM images were believed to be the aggregates formed by POSS-AH and PAA chains. During the PAA free radical polymerization process, POSS-AH particle contains a large number of hydroxyl and amino groups caused PAA chains to aggregate and form micelles by hydrogen bonds and ionic interactions. These POSS-AH nanoparticals acted as multifunctional crosslinks. The micelles aggregated spontaneously to form clusters. The small clusters (Fig. 3a) grew up and connected with each other (Fig. 3b) then the big flower-shaped spheres were formed (Fig. 3c).

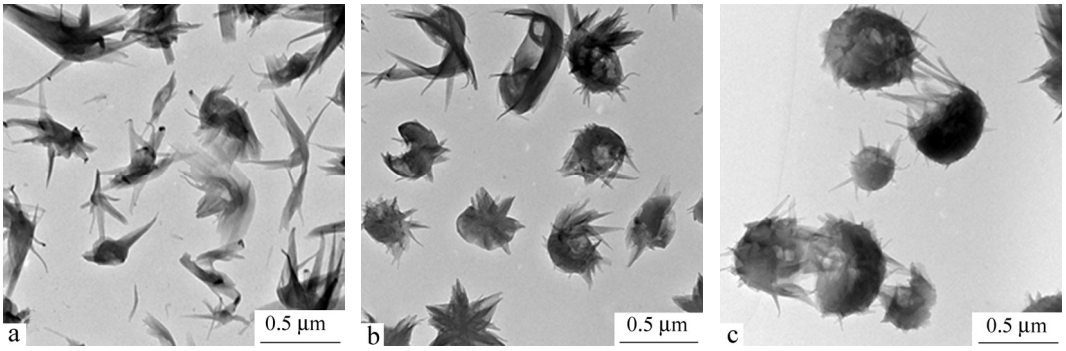

Fig. 3 TEM images of sample P50B50

A schematic illustration of the dual network formation process is shown in Fig. 4. In the PAA/POSS-AH clusters, the PAA chains and POSS-AH form physical crosslinks through hydrogen bonds and ionic interactions. Among the clusters, the polymer chains form covalent crosslinks through Bis. When the hybrid hydrogel was stretched, some of these clusters deformed and untied progressively and absorbed a large amount of energy. Therefore the hydrogel exhibits high stretch ability and notch-insensitive properties.

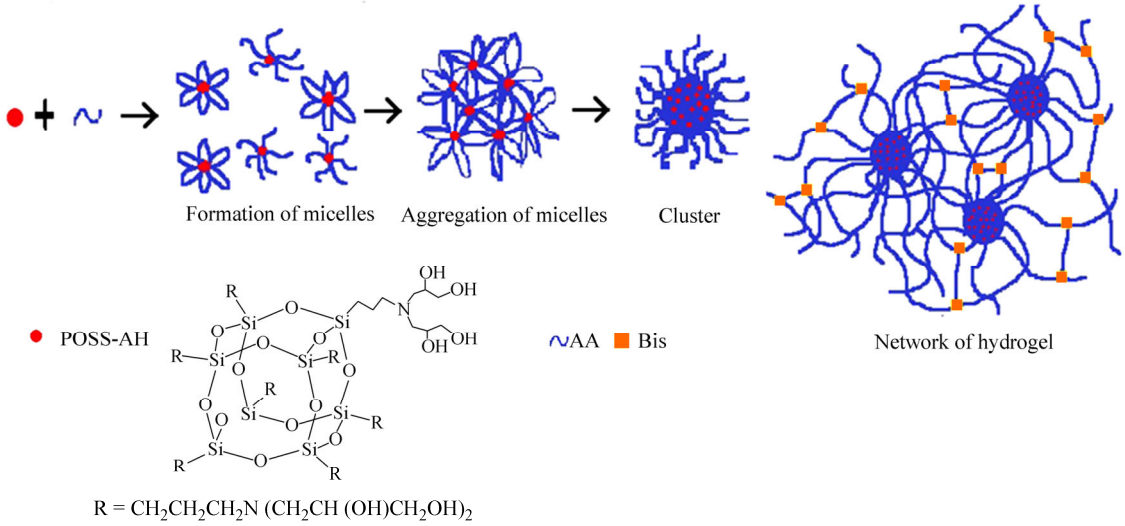

Fig. 4 Schematic illustration of the dual network formation process

Self-healing Ability

This hydrogel was also endowed with self-healing ability by the reversible physical crosslinks. Figure 5 illustrates the self-healing behavior after being cut off and maintained in a closed vessel at 37 °C for 48 h. The interface in the bulk disappeared almost completely and the sample can withstand a large extension without broken.

Tensile tests were performed on the original and self-healed samples to further quantitatively evaluate the self-healing property. Three factors, including the POSS-AH content, AA monomer concentration and neutralization degree of AA, had significant effects on the self-healing process. Here the hydrogel samples were divided to three groups denoted as P*x*, A*y*, N*z* respectively, and the reactant compositions are listed in Table 1.

The tensile test results of group P (Fig. 6a) illustrated the effect of POSS-AH on self-healing process. When 5 wt% (relative to AA) POSS-AH was used, about 50% recovery of tensile strength was achieved after healing for 24 h. When the concentration of POSS-AH increased to 10 wt% (relative to AA) the recovery of tensile strength decreased to 20%. We speculate that the flexible chain lengths at the cut surface decreased with the increasing POSS-AH, which led to the decrease of the self-healing ability of the hydrogels.

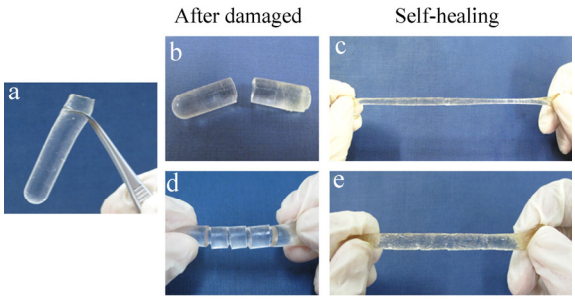

Fig. 5 Photographs of self-healing behavior of sample P5: (a) the original hydrogel; (b, d) the hydrogel after cutting; (c, e) the hydrogel after self-healing

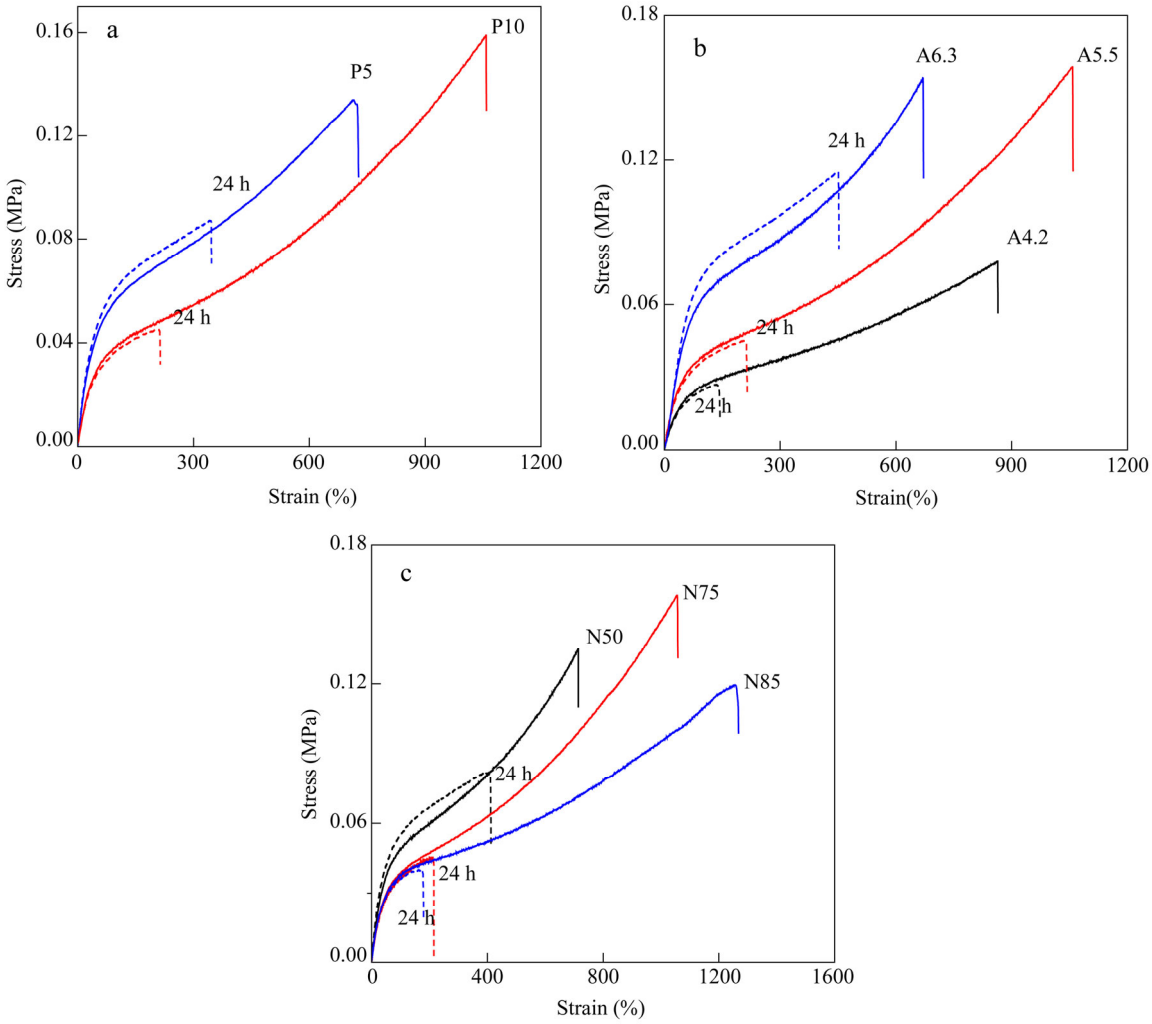

Fig. 6 The self-healing properties of the hydrogels: (a) effects of POSS-A content on the recovery of tensile strength of self-healed hydrogels; (b) effects of AA concentration on the recovery of tensile strength of self-healed hydrogels and (c) effects of neutralization degree on the recovery of tensile strength of self-healed hydrogels

Samples in group A with various initial concentrations of AA (Fig. 6b) showed that there was a significant effect on healing ability with increasing the monomer concentration in the reactive system at the start of the reaction. The polymer concentration generally increases with an increase in the monomer concentration.

Accordingly, the level of macromolecular entanglement increased and the mechanical strength of the hydrogel was significantly improved. A sufficient amount of long polymer chains on the cut surfaces is a decisive factor for the self-healing process[34]. The neutralization degree of AA also played an important role in this system. Figure 6(c) showed the relationship between the self-healing efficiency and the neutralization degree of AA. As the neutralization degree increased by adding NaOH, the self-healing ability decreased. Neutralization converted the hydrogen bonding in PAA and resulted in the reduction of mechanical strength and self-healing ability. In this study the hydrogel was prepared for biomedical applications, so the purpose of neutralization was to maintain the pH value of the system match the requirement of the physiological environment.

Swelling and Water Retention Behavior

Swelling behavior is one of the most important factors of a hydrogel because it is correlated with many essential properties, such as permeability, mechanical characteristics and biocompatibilities[35, 36]. The swelling ability of the PAA/POSS-AH hydrogels is illustrated in Fig. 7. An increase in the ionic strength led to a decrease in the water uptake. Because the increase in ionic strength caused changes of the polymer chain conformation, the polymer chains extended more in deionized water as the ionic groups in the macromolecule repelled each other.

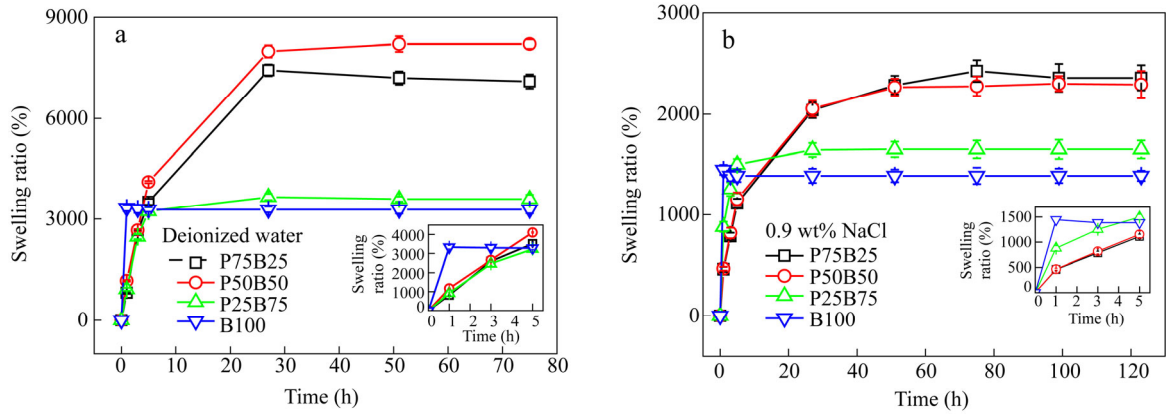

Fig. 7 Swelling ratios of the hydrogels in (a) deionized water and (b) normal saline solution

The equilibrium swelling ratio of the hydrogel was significantly enhanced as POSS-AH was introduced into the network. For sample P100 the hydrogels dissolved both in deionized water and normal saline solution after 24 h. This indicated that during the swelling process the physical crosslink between PAA and POSS-AH disbanded gradually. In deionized water the equilibrium swelling ratio of sample P50B50 was slightly higher than that of sample P75B25, and there was a decrease in the swelling ratio of sample P75B25 with time after 30 h. This is attributed to the small amount of hydrogel dissolution in sample P75B25 caused by disbanded physical crosslinks.

At the beginning of swelling, sample B100 absorbed water very rapidly and swelled to an equilibrium state in less than 1 h. However, the sample containing POSS-AH swelled relatively slowly and the time for dried hydrogels to reach swelling equilibrium was about 30 h in deionized water and 80 h in normal saline solution.

The deswelling behavior of fully swollen hydrogel was shown in Fig. 8. The POSS-AH content significantly affected the water retention ability of the hydrogels. The sample with more POSS-AH showed excellent water retention ability. POSS-AH brought a large amount of hydrophilic groups. Thereby, hydrogen bonds readily developed interactions between the crosslink network and water molecules.

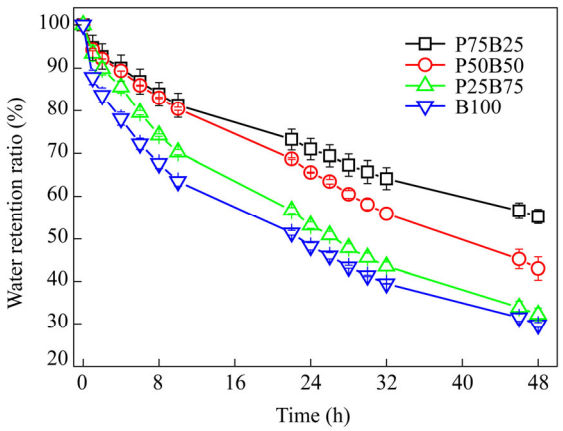

Fig. 8 Hydrogel deswelling kinetics at 20 °C and 80% relative humidity

CONCLUSIONS

Our data suggested that the POSS-AH nanoparticle was an effective crosslinker for PAA polymers. The mechanical properties of the hydrogels could be controlled over a wide range by the ratio of physical crosslink versus chemical crosslink. The combination of high stretchability, notch insensitivity and self-healing, along with an easy method of synthesis, made these materials ideal candidates for further applications.

REFERENCES

1 Ono, T., Sugimoto, T., Shinkai, S. and Sada, K., Nat. Mater., 2007, 6: 429
2 Hoffman, A.S., Adv. Drug Deliver. Rev., 2012, 64: 18
3 Wang, L., Ren, J., Yao, M., Yang, X., Yang, W. and Li, Y., Chinese J. Polym. Sci., 2014, 32(12): 1581
4 Artzi, N., Zeiger, A., Boehning, F., bon Ramos, A., van Vliet, K. and Edelman, E.R., Acta Biomater., 2011, 7: 67
5 Zhao, Z., An, S., Xie, H. and Jiang, Y., Chinese J. Polym. Sci., 2015, 33(1): 173
6 Qiu, Y., and Park, K., Adv. Drug Deliver. Rev., 2012, 64: 49
7 Cui, J., Lackey, M.A., Madkour, A.E., Saffer, E.M., Griffin, D.M., Bhatia, S.R., Crosby, A.J. and Tew, G.N., Biomacromolecules, 2012, 13: 584
8 Brown, H.R., Macromolecules, 2007, 40: 3815
9 Gong, J.P., Katsuyama, Y., Kurokawa, T. and Osada, Y., Adv. Mater., 2003, 15: 1155
10 Sun, J.Y., Zhao, X., Illeperuma, W.R.K., Chaudhuri, O., Oh, K.H., Mooney, D.J., Vlassak, J.J. and Suo, Z., Nature, 2012, 489: 133
11 Huang, T., Xu, H., Jiao, K., Zhu, L., Brown, H.R. and Wang, H., Adv. Mater., 2007, 19: 1622
12 Haraguchi, K. and Takada, T., Macromolecules, 2010, 43: 4294
13 Hager, M.D., Greil, P., Leyens, C., van der Zwaag, S. and Schubert, U.S., Adv. Mater., 2010, 22: 5424
14 Lehn, J.M., Proceedings of the National Academy of Sciences of the United States of America, 2002, 99: 4763
15 Deng, G., Li, F., Yu, H., Liu, F., Liu, C., Sun, W., Jiang, H. and Chen, Y., ACS Macro. Lett., 2012, 1: 275
16 Phadke, A., Zhang, C., Arman, B., Hsu, C.C., Mashelkar, R.A., Lele, A.K., Tauber, M.J., Arya, G. and Varghese, S., Proceedings of the National Academy of Sciences, 2012, 109: 4383
17 Zhang, M., Xu, D., Yan, X., Chen, J., Dong, S., Zheng, B. and Huang, F., Angew. Chem., 2012, 124: 7117
18 Harada, A., Kobayashi, R., Takashima, Y., Hashidzume, A. and Yamaguchi, H., Nat. Chem., 2011, 3: 34
19 Tuncaboylu, D.C., Sari, M., Oppermann, W. and Okay, O., Macromolecules, 2011, 44: 4997
20 Cong, H., Wang, P. and Yu, S., Chem. Mater., 2013, 25: 3357
21 Cui, W., Zhang, Z., Li, H., Zhu, L., Liu, H. and Ran, R., RSC Adv., 2015, 5: 52966

22 Cui, W., Ji, J., Cai, Y., Li, H. and Ran, R., J. Mater. Chem. A, 2015, 3: 17445
23 Kuo, S.W. and Chang, F.C., Prog. Polym. Sci., 2011, 36: 1649
24 Leitner, V.M., Marschutz, M.K. and Bernkop-Schnurch, A., Eur. J. Pharm. Sci., 2003, 18: 89
25 Hu, X., Wei, W., Qi, X., Yu, H., Feng, L., Li, J., Wang, S., Zhang, J. and Dong, W., J. Mater. Chem. B, 2015, 3: 2685
26 Wei, Z., He, J., Liang, T., Oh, H., Athas, J., Tong, Z., Wang, C. and Nie, Z., Polym. Chem., 2013, 4: 4601
27 Gulyuz, U. and Okay, O., Macromolecules, 2014, 47: 6889
28 Zhang, W. and Müller, A.H.E., Prog. Polym. Sci., 2013, 38: 1121
29 Mori, H., Lanzendorfer, M.G., Müller, A.H.E. and Klee, J.E., Macromolecules, 2004, 37: 5228
30 Lu, L., Zhang, C., Li, L. and Zhou, C., Carbohyd. Polym., 2013, 94: 444
31 Mori, H., Müller, A.H.E. and Klee, J.E., J. Am. Chem. Soc., 2003, 125: 3712
32 Yu, Q. M., Tanaka, Y., Furukawa, H., Kurokawa, T. and Gong, J.P., Macromolecules, 2009, 42: 3852
33 Sanchez, C., Soler-Illia, G.J.d.A.A., Ribot, F., Lalot, T., Mayer, C.R. and Cabuil, V., Chem. Mater., 2001, 13: 3061
34 Zhang, H., Xia, H. and Zhao, Y., ACS Macro Lett., 2012, 1: 1233
35 Park, H., Guo, X., Temenoff, J.S., Tabata, Y., Caplan, A.I., Kasper, F.K. and Mikos, A.G., Biomacromolecules, 2009, 10: 541
36 Zhang, H., Zhao, C., Cao, H., Wang, G., Song, L., Niu, G., Yang, H., Ma, J. and Zhu, S., Biomaterials, 2010, 31: 5445